JOURNAL OF SOLID STATE CHEMISTRY 52, 233–243 (1984)

Magnetic Properties of Iron-Intercalated Titanium Diselenide

D. R. HUNTLEY* AND M. J. SIENKO†

Baker Laboratory of Chemistry, Cornell University, Ithaca, New York 14853

AND K. HIEBL

Institut fur Physikalische Chemie, Vienna, Austria

Received September 19, 1983

Powder samples of Fe_xTiSe_2 ($0.00 \leq x \leq 0.50$) have been prepared by direct reaction of high purity elements. Crystal parameters were determined by the Debye–Scherrer powder diffraction technique. Magnetic susceptibility measurements were made by the Faraday method in the temperature range 1.5–300 K and indicated magnetic odering for compositions with $x > 0.03$. The magnetic ordering temperature, T_m, was observed to move to higher temperature with increasing iron concentration. These results have been interpreted in terms of a spin-glass model for low iron concentrations ($x < 0.2$) and antiferromagnetism for high concentrations ($x > 0.2$).

Introduction

The structure of the transition metal dichalcogenides consists of a hexagonal array of metal atoms surrounded by two hexagonal sheets of chalcogen atoms. In the case of $TiSe_2$ (Fig. 1), the selenium sheets are arranged to give octahedral coordination about the titanium atoms. These individual layers are stacked such that the titanium atoms lie directly over each other along the crystallographic c axis. The bonding within the layers is quite strong, while the bonding between the layers is weak, consisting of van der Waals interactions between the selenium atoms. Various atomic or molecular species can be inserted or intercalated into the van der Waals gap, including alkali metals, organic and organometallic compounds, and transition metals (*1*). In this paper we deal exclusively with the properties of transition metal intercalates.

The electronic properties of $TiSe_2$ are determined by the band structure, which has been the subject of some controversy (*2*). The titanium in $TiSe_2$ is formally in the 4^+ oxidation state, and has no d electrons, hence it should be an insulator. However, $TiSe_2$ has metallic conductivity (*3*). The high conductivity can be explained either by a slight nonstoichiometry ($Ti_{1+x}Se_2$) giving rise to a high defect conductivity or by overlap of the titanium d band with the selenium p band resulting in semimetallic behavior. Each intercalated transition metal donates 2 or 3 electrons to the titanium t_{2g} band, which in the simple rigid band scheme, should increase the conduction electron concentration and hence the conductivity. Just the opposite is observed, with increasing iron content in $TiSe_2$, the conductivity decreases, presumably due to scattering by the magnetic ions (*4*).

* To whom correspondence should be addressed at Chemistry Division, Oak Ridge National Laboratory, Oak Ridge, TN 37830.

† Deceased.

0022-4596/84 $3.00

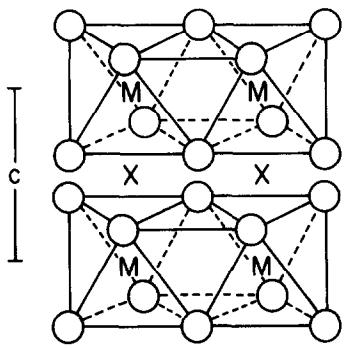

FIG. 1. Structure of 1T $TiSe_2$. M = Ti; ○ = Se; X = octahedral interstices. The hexagonal a parameter is defined as the Ti–Ti distance within the layer. The hexagonal c parameter is defined as the Ti–Ti distance perpendicular to the layer.

It is doubtful that the rigid band model is appropriate to these systems. Recent studies (*5*) have suggested that the rigid band model is inadequate to explain the observed physical properties of lithium-intercalated ZrS_2. In the transition metal intercalates the bonding interactions between the intercalated atom and the chalcogens are comparable to the bonding between the host metal and the chalcogens and therefore, the material is significantly less two-dimensional. The rigid band scheme fails to account for these changes in the bonding.

A substantial amount of work has been reported on transition metal-intercalated niobium and tantalum dichalcogenides, where the transition metal is vanadium, chromium, manganese, iron, cobalt, or nickel (*6–8*). The structure of the niobium and tantalum dichalocogenides is similar to that of $TiSe_2$ except that the chalcogen sheets are arranged to yield trigonal prismatic coordination about the metal. Generally in these systems, the structure of the host transition metal dichalcogenide remains intact and the intercalated transition metal ions occupy the octahedral interstices between the layers.

For the Ti, V, and Cr intercalates, the ions are apparently in the 3+ oxidation state, while for the Mn, Fe, Co, and Ni intercalates, the ions are 2+. This information comes primarily from careful magnetic studies carried out on powders as well as on single crystals. Most of the studies were done on materials with "special" compositions, e.g., $M_x TX_2$ where x = 1/4, 1/3, or 1/2. These compositions are special because they form crystallographically ordered structures. Further evidence of the valence states comes from lattice parameter data. When plotted versus atomic number, the c parameter (the lattice distance perpendicular to the layers) for the system $M_{1/3}TaS_2$ shows a discontinuous jump between Cr and Mn, which Parkin and Friend interpret as a change in valence state from 3+ to 2+. X-Ray photoemission measurements and Mössbauer spectroscopy have confirmed the presence of Mn^{2+} and Fe^{2+} in selected systems (*8, 9*).

These materials are magnetically interesting since many undergo ordering phenomena, which is often surprisingly different for very similar materials. For example, $Fe_{0.33}TaS_2$ is a ferromagnet with a Curie temperature of 35 K while $Fe_{0.33}NbS_2$ is an antiferromagnet with a Nèel temperature of 46 K (*6*). Table I summarizes some recent

TABLE I

Compound	T_m (K)	Type of ordering	μ_{Fe}	Reference
$Fe_{1/4}NbS_2$	137	AFM	4.7	(*8*)
$Fe_{1/3}NbS_2$	47	AFM	4.8	(*8*)
$Fe_{1/3}NbS_2$	45	AFM	6.3	(*6*)
$Fe_{0.05}NbSe_2$			3.2	(*11*)
$Fe_{0.10}NbSe_2$	7.6	AFM	3.3	(*12*)
$Fe_{1/3}NbSe_2$	135	AFM	4.6	(*12*)
$Fe_{1/3}TaS_2$	3.5	FM	6.4	(*6*)
$Fe_{0.05}TaSe_2$	2.0	AFM	2.9	(*11*)
$Fe_{0.10}TaSe_2$	12	AFM	3.6	(*11*)
$Fe_{1/2}TiS_2$	111	FM	4.8	(*14*)
$Fe_{2/3}TiS_2$	112	FM	3.2	(*14*)
$Fe_{0.34}TiSe_2$	113	AFM	4.1	(*15*)
$Fe_{1/2}TiSe_2$	134	AFM	3.6	(*16*)

magnetic susceptibility results on some related systems.

The concentration dependence of the magnetic phenomena in Fe_xTaS_2 (*10, 11*), Fe_xTaSe_2 (*10, 11*), and Fe_xNbSe_2 (*11, 12*) has been reported. The results have been interpreted within the framework of the destruction of the charge density wave and the transition from a spin-glass to a state with long range magnetic order. The magnetic, electrical, and structural properties of M_xTiS_2 (M = Fe, Co, Ni) have been reported for x = 0.25, 0.33, 0.40, 0.50, 0.75 (*13*), and x = 0.67 (*14*). Lyding *et al.* have recently published the crystal structure of $Fe_{0.34}TiSe_2$ (*15*) and transport properties of Fe_xTiSe_2 (*4*). The magnetic susceptibility of $Fe_{0.50}TiSe_2$ has also been reported (*16*). Structural work on the series M_xTiSe_2 (M = Fe, Co, Ni) has been reported by Arnaud *et al.* (*17*). However, relatively few systematic studies relating the concentration dependence of the magnetic properties in transition metal-intercalated group IV transition metal dichalcogenides have been completed. In this study, the concentration dependence of the magnetic properties of Fe_xTiSe_2 is examined.

Experimental

Samples of Fe_xTiSe_2 ($0.0 < x < 0.5$) were prepared by direct reaction of high purity titanium wire (Materials Research Corp., MARZ grade), iron wire (Materials Research Corp., MARZ grade), and selenium shot (99.9999%, Atomergic Chemetals Corp.). Stoichiometric quantities of the elements were weighed into previously degassed fused silica sample tubes. The samples were sealed under vacuum (10^{-6} Torr) and placed in a furnace with a flat temperature gradient. The samples were heated to 400°C for 4 days to prereact the elements before increasing the temperature to 750°C. After 7 days at this temperature, the samples were slowly cooled to room temperature and thoroughly ground with an agate mortar and pestle in a helium atmosphere Dri-Lab to assure homogeneity. The ground samples were loaded into previously outgassed sample tubes and again sealed under vacuum. The samples were reacted again at 750°C for 10 to 14 days. The resulting materials were all microcrystalline powders. The samples changed color from red–violet to black as the iron content was increased. The samples were somewhat moisture sensitive, liberating H_2Se when exposed to air, and were therefore stored in a helium atmosphere Dri-Lab.

Powder X-ray diffraction patterns of the samples were obtained with a 114.6-mm-diameter Debye–Scherrer camera using nickel–filtered copper $K\alpha$ radiation. Line positions were obtained by a microprocessor-controlled densitometer and were corrected for film shrinkage by the Straumanis method. Errors due to sample absorption and beam divergence were corrected by the Bradley–Jays method (*18*). Lines were indexed with the aid of a computer program (*19*) which calculates line intensity and positions of possible reflections based on available crystal structure data for $TiSe_2$. Lattice parameters were refined using Cohen's method of least squares (*18*). All samples appeared single phased to X-ray analysis. However, for samples with concentrations above x = 0.25, the diffraction lines were broadened.

Magnetic susceptibilities were measured in a helium atmosphere from 1.5 to 300 K by the Faraday method with use of the apparatus described elsewhere (*20*). The balance was calibrated using $HgCo(SCN)_4$ as a standard. The susceptibilities were measured as a function of field strength between approximately 2 and 12 kG. The reported susceptibilities have been corrected for the susceptibility of the Spectrosil quartz sample bucket.

The field-cooling experiments were carried out by applying a field of 5000–10,000

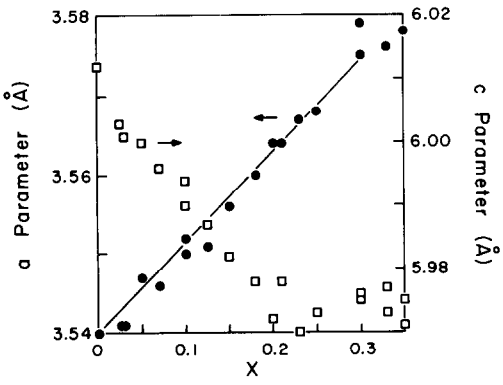

FIG. 2. Lattice parameters vs composition in Fe_xTiSe_2. Circles, hexagonal a parameter. Squares, hexagonal c parameter.

G and cooling the sample slowly through T_m. The measured susceptibility was allowed to stabilize at low temperature (this took approximately 1 hr). The field was turned down to 0 G and the susceptibility was measured as usual.

High-temperature magnetic susceptibility measurements were performed over the temperature range 300–600 K on samples with iron compositions $x = 0.10$, 0.25, and 0.33 with a pendulum susceptibility meter by using a compensation Faraday method under pure argon (*21*).

Electron spin resonance measurements were made on a Varian E-12 spectrometer. No signals were observed between 10 and 300 K.

Results and Discussion

X-Ray Analysis

The powder X-ray patterns for all samples were indexed based on the $TiSe_2$ structure. The $TiSe_2$ prepared in this study is very close to the ideal stoichiometry as evidenced by the lattice constants. The experimental values of a and c (3.540 and 6.008 Å, respectively) are to be compared with the literature values of 3.540 and 6.008 obtained from neutron diffraction (*22*). Figure 2 summarizes the effect of iron doping on the hexagonal a and c parameters. The lattice constants extrapolate at $x = 0.00$ to the reported values for $TiSe_2$ (*22*), and no gross structural changes were observed over the whole concentration range studied. These data suggest that the iron is indeed occupying interstitial sites in the van der Waals gap and not substituting for the titanium in the layers.

The hexagonal a parameter increases linearly with composition due to an increased Coulombic repulsion caused by the donation of electrons from the iron to the nonbonding d bands of the titanium. The behavior of the hexagonal c parameter depends on two competing factors: the increased interlayer repulsion due to the additional electron density donated by the iron atoms and the increased interlayer attraction due to the presence of a positively charged ion in the van der Waals gap. At low iron concentration, $x \leq 0.2$, the pinning of the layers due to the positively charged iron dominates and the c axis contracts slightly. At higher iron concentration, the interlayer repulsion cancels the attractive effect of the intecalated iron, and the c axis remains relatively constant. The unit cell volume increases linearly with iron concentration.

Magnetic Susceptibility Results

In iron-intercalated $TiSe_2$, the iron d levels are close in energy to the titanium d bands, and hence, it is not obvious whether the iron d electrons should remain localized on the iron atoms or become delocalized into the $TiSe_2$ conduction band. The magnetic susceptibility results presented here indicate the presence of localized moments on the iron atoms. The temperature dependence of the magnetic susceptibility for a few representative samples is shown in Fig. 3. For samples with $x > 0.03$, there is a well-defined maximum in the susceptibility, characteristic of antiferromagnetic order-

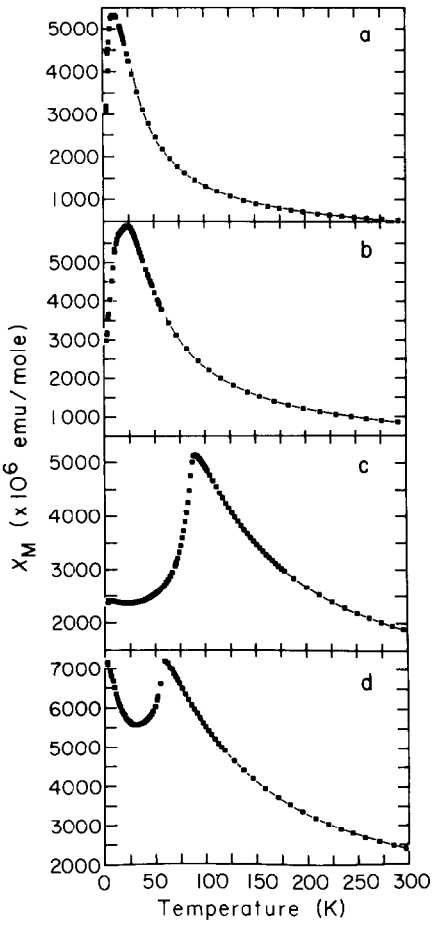

FIG. 3. Temperature dependence of the molar magnetic susceptibility for (a) $Fe_{0.05}TiSe_2$, (b) $Fe_{0.10}TiSe_2$, (c) $Fe_{0.22}TiSe_2$, and (d) $Fe_{0.33}TiSe_2$. The solid line indicates the calculated curve based on the fitted parameters. In all cases, the susceptibility was measured in an applied field of approximately 10,850 G, and some high-temperature data points were omitted from the graph for clarity.

ing. The temperature at which the maximum occurs, T_m, generally increases with increasing iron concentration. The only exception is for $x = 0.33$ which will be discussed later in the text. As shown in Fig. 4, the initial rise in T_m is smooth, however, at $x = 0.20$, there is a discontinuity which is interpreted as a changeover from a spin-glass state to an antiferromagnetic regime.

For this system, the magnitude of the magnetic susceptibility is due to several contributions; the Curie–Weiss behavior of the local moments, the Pauli paramagnetism and the Landau diamagnetism of the conduction electrons, the diamagnetism due to the ion cores and a contribution due to the interaction of the local moments with the conduction electrons and with each other. The magnetic data obtained in this study were fitted (using a nonlinear least-squares fitting routine originally written by Bevington (*23*)) to a modified Curie–Weiss law:

$$X = C/(T - \theta) + X_0 \qquad (1)$$

where X is the observed susceptibility, C is the Curie constant, T is the absolute temperature, θ is the Weiss constant, and X_0 is a temperature independent term which includes the Pauli paramagnetism and the Landau and core diamagnetism. In order to obtain consistent values of the fitted parameters, it was necessary to fit only data at temperatures well above the ordering temperature, T_m, hence all data were fitted from 2.5 T_m to room temperature. In order

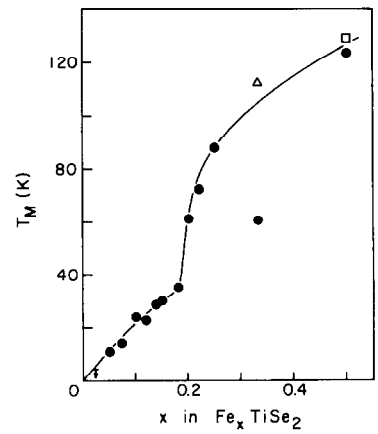

FIG. 4. The magnetic ordering temperature, T_m, vs composition in Fe_xTiSe_2. Circles indicate the current work; the triangle represents the data of Lyding *et al.* (*15*); the square represents the data of Muranaka *et al.* (*16*).

TABLE II

x	T_m (K)	μ_{Fe}	θ (K)	χ_0[a] ($\times 10^{-6}$ emu mole)
0.03	—	4.3	−3.2	109
0.05[b]	11	4.4	−2.0	128
0.07	14	4.2	−4.3	111
0.10	24	4.2	−1.5	127
0.15	30	4.2	−3.1	185
0.20	62	4.0	−0.3	287
0.22	72	3.9	+2.8	247
0.25	89	3.9	+3.5	277
0.30	85	4.1	−19.1	252
0.33[b]	60	4.0	−34.0	327
0.35	60	4.0	−33.7	304

[a] Corrected for the diamagnetism of the ion cores (*24*).

[b] Fit to 600 K.

to avoid complications due to the non-Curie law behavior near the ordering temperature, the susceptibilities were measured and fit to 600 K for samples with $x = 0.05$, 0.25, and 0.3. The results of the fitting are summarized in Table II. The quality of the fits was excellent as indicated in Fig. 3.

The average magnetic moment per mole of iron in Fe_xTiSe_2 is 4.2 μ_B. This moment is in general agreement with the moments found in the literature for related systems (see Table I). The moment obtained from the susceptibility is best interpreted as high-spin iron II (spin only moment of 4.9 μ_B). The reduction in moment is due either to an interaction with the $TiSe_2$ conduction electrons or strong covalent interactions with the selenium.

The presence of high-spin iron II is also confirmed by Mössbauer spectroscopy done on $Fe_{0.20}TiSe_2$ (*25*). The room temperature isomer shift is 0.73+/−0.01 mm/sec which is in the range of Fe^{2+} compounds (*26*). The linewidth is rather broad, indicative of more than one iron site in this compound, which is expected for a composition which does not form a crystallographically ordered structure since the iron atoms do not occupy unique positions. The values for the isomer shift are nearly identical to those reported (*26*) for the analogous Fe_xTiS_2 system.

Discussion

As discussed in the introduction, $TiSe_2$ is metallic due either overlap of the Se p band with the Ti d band or to interstitial Ti^{3+} ions. The introduction of magnetic ions into a metallic host has many interesting consequences due to the interaction of the localized moment with the conduction electrons. There have been a large number of studies relating to the magnetic properties of transition metal/noble metal alloys (e.g., Fe*Au*). [For reviews see Refs. (*27, 28*).] Like the transition metal dichalcogenides, these systems offer the opportunity to examine magnetic behavior as a function of magnetic ion concentration. The properties of dilute magnetic alloys can be divided into several regimes. In the extremely dilute solutions, the magnetic moments are noninteracting, but are reduced by a Kondo spin-flip mechanism due to the scattering of the conduction electrons by the magnetic impurities. At somewhat higher concentration, the spin-glass regime, the moments interact directly with each other over long distances, usually by an interaction with the conduction electrons. As the concentration is increased further, clusters of local magnetic order can form, but these clusters can interact as individual moments in a spin-glass matrix. Eventually, a percolation limit is reached, where the moments can interact directly and long range order is achieved.

A spin-glass exhibits a maximum in the magnetic susceptibility at a well-defined temperature, T_m. This can be understood in terms of the random spatial distribution of magnetic ions in the host lattice. The sign of the interaction of the moments varies with distance and is oscillatory (e.g., RKKY interaction or spin density wave). Hence, a random spatial distribution of moments will

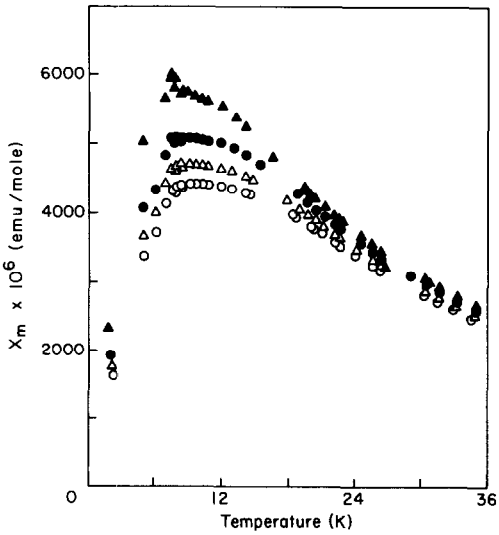

FIG. 5. The field dependence of the magnetic susceptibility for $Fe_{0.05}TiSe_2$. The approximate fields are open circles = 10,850 G; open triangles = 7200 G; filled circles = 4800 G; filled triangles = 2400 G.

result in a random set of parallel and antiparallel interactions. The resulting system has an infinite number of degenerate or nearly degenerate low energy states and is nonmagnetic. At T_m, the spin–spin interaction energy is greater than the thermal energy, and the system freezes into some nonmagnetic state. Above, T_m, thermal energy dominates and the material behaves as a normal paramagnet.

The shape of the susceptibility maximum depends on the strength of the applied magnetic field used to measure the susceptibility. Since the moments are only weakly frozen, an applied magnetic field will tend to align the spins. The shape of the susceptibility maximum reflects this; for high applied fields, the maximum is depressed and broadened, but for low fields, the maximum is sharper and more well defined.

The field dependence of the susceptibility maxima is shown in Fig. 5 for a sample of low concentration ($x = 0.05$) and in Fig. 6 for a sample of high concentration ($x = 0.25$). A very strong field dependence is observed for the low concentration ($x = 0.05$) sample, with the lowest field yielding the largest susceptibility and the sharpest maximum. The field dependence decreases above the maximum and at room temperature the susceptibility is field independent. For comparison, the field dependence near the maximum is shown for the high-concentration ($x = 0.25$) sample. As shown, there is no systematic field dependence for the higher concentration sample.

The spin-glass state has been the subject of many theoretical papers (*28–31*). Sherington and Kirkpatrick (*30*) apply mean field theory and obtain a "spin-glass order parameter" q, which is defined as

$$q(T) = \langle |\langle S_i \rangle_T|^2 \rangle_r \qquad (2)$$

which can be interpreted as a thermally averaged localized moment, which has been squared to remove the orientation dependence and then spatially averaged. For a frozen spin system ($T < T_m$), $q(T)$ is finite; for a dynamic spin system ($T > T_m$), $q(T)$ is zero. The order parameter can be ex-

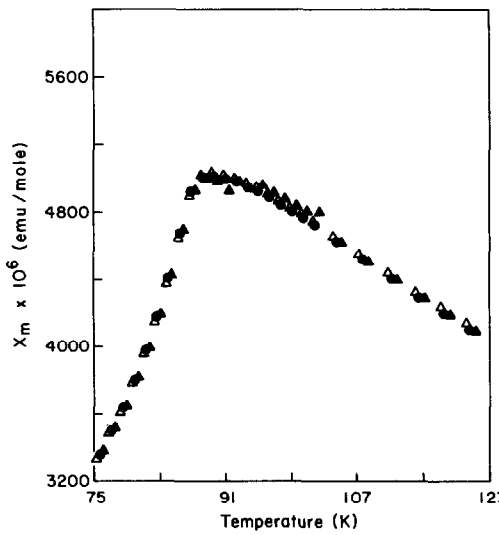

FIG. 6. The field dependence of the magnetic susceptibility for $Fe_{0.25}TiSe_2$. The symbols for the magnetic field values are the same as in Fig. 5.

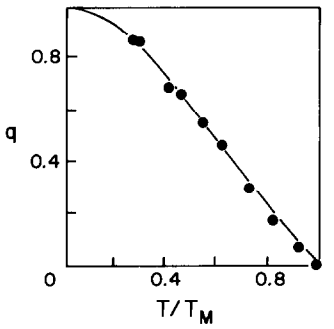

FIG. 7. The spin-glass order parameter for $Fe_{0.05}TiSe_2$, compared with the mean field prediction of Thouless *et al.* (*31*).

pressed in terms of the susceptibility parameters as (*12*)

$$q(T) \approx 1 - \frac{T\chi(T)}{C(T_m) + \theta(T_m)\chi(T)} \quad (3)$$

In Fig. 7, the order parameter calculated from the susceptibility data for the sample with $x = 0.05$ is compared with the mean field prediction of Thouless *et al.* (*31*).

Since the spin-glass system is characterized by a multiplicity of ground states, the configuration of the spins at the freezing temperature will depend on the history of the experiment. If a sample is cooled to low temperatures in the absence of an external applied magnetic field, the resulting glass will be nonmagnetic. If, however, the sample is cooled in the presence of an applied field, the sample should freeze with some net magnetic moment since the field will act to align the spins ferromagnetically as they freeze. The behavior of $Fe_{0.10}TiSe_2$ under field cooling experiments is shown in Fig. 8.

The temperature dependence of the susceptibility below T_m is in general agreement with the predictions of the spin-glass model. The field dependence of the field-cooled susceptibility is that of a ferromagnet with the lowest field yielding the highest value of the susceptibility. The low-temperature value of the susceptibility under these conditions depends strongly on the applied field. In Fig. 9, the susceptibility of $Fe_{0.07}TiSe_2$ cooled in fields of 0, 4800, and 10,850 G is shown. The field-cooled susceptibility is highest for the largest applied field due to an increase in the magnetization.

One interaction which couples magnetic moments over large distances is the Ruderman–Kittel–Kasuya–Yosida (RKKY) interaction. The localized moments polarize the conduction electron gas, which in turn interacts with a second moment. In this way, spins separated by large distances can be coupled. This exchange interaction is expressed by

$$J(r) \propto \frac{\sin 2k_f r}{(2k_f r)^4} - \frac{\cos 2k_f r}{(2k_f r)^3}$$

where r is the distance separating the moments and k_f is the Fermi wavevector. The interaction is oscillatory so that the spin alignment can be parallel or antiparallel. Although the strength of the interaction depends inversely on the separation of the spins, the RKKY interaction can couple spins over large distances. Conductivity

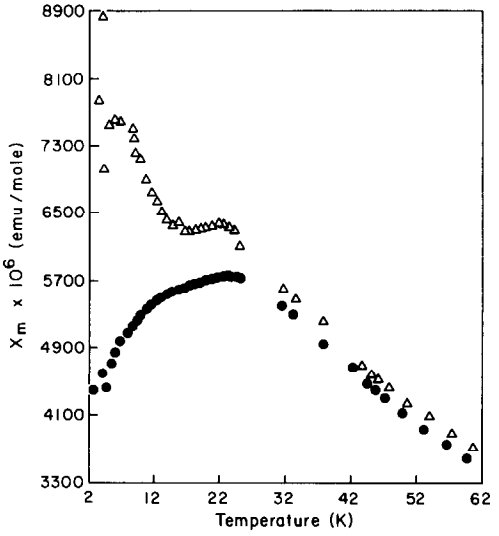

FIG. 8. Magnetic susceptibility after cooling in an external magnetic field of 4800 G for $Fe_{0.10}TiSe_2$. The susceptibility was measured in fields of approximately 10,850 G (circles) and 2400 G (triangles).

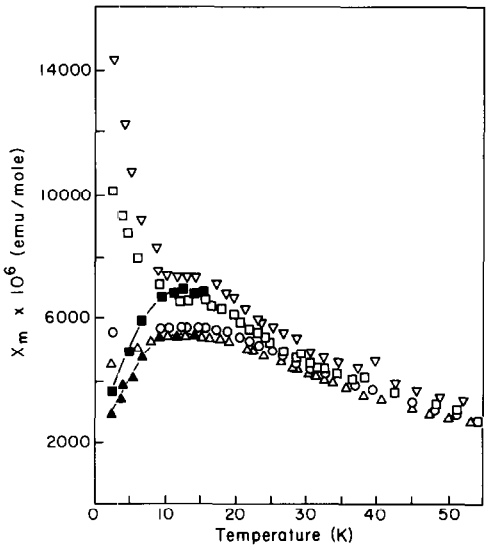

FIG. 9. Magnetic susceptibility of $Fe_{0.07}TiSe_2$, under the following conditions: closed triangles: cooled in zero external field, measured in an applied field of 10,850 G; closed squares: cooled in zero external field, measured in an applied field of 2400 G; open triangles: (△) cooled in an external field of 4800 G, measured in an applied field of 10,850 G; open squares: cooled in an external field of 4800 G, measured in an applied field of 2400 G; open circles: cooled in an external field of 10850 G, measured in an applied field of 10,850 G; inverted triangles: cooled in an external field of 10,850 G, measured in an applied field of 2400 G.

and Hall measurements (*4, 15*) on Fe_xTiSe_2, indicate that there is substantial interaction between the conduction electrons and the localized magnetic moments. These data suggest that the RKKY mechanism probably does play some role in the magnetic properties of this material.

Another possible mechanism of coupling involves superexchange via the chalcogen atoms. Even at high concentration, the intercalated iron atoms are separated by approximately 7.5 Å which is too far for direct overlap of the $3d$ wavefunctions. It seems likely therefore, that superexchange plays an important role in establishing long range order in these compounds. For dilute samples it is possible to have very weak superexchange interactions through a large number of chalcogen atoms and, in fact, to have both ferromagnetic and antiferromagnetic alignment. This would result in a "superexchange spin-glass" and would exhibit properties similar to the more common RRKY glasses.

The third mechanism of coupling is through spin density wave (SDW) formation. Overhauser was the first to propose SDW as a mechanism of antiferromagnetism in dilute alloys (*32*). More recently, Antoniou (*33*) has shown that SDWs are stabilized by magnetic impurities especially in systems which undergo charge density wave (CDW) transitions. The properties of Fe_xTaSe_2 (*33*) may be interpreted as simultaneous destruction of the CDW and formation of a SDW. $TiSe_2$ also undergoes a CDW transition (*3*) at approximately 200 K and may be expected to stabilize a SDW in the presence of intercalated iron. Hilenius has suggested a "SDW spin-glass" as an interpretation for the properties of Fe_xNbSe_2 (*11*). Antoniou (*33*) distinguishes a SDW glass from a conventional spin-glass on the basis of field-cooling experiments. In a SDW spin-glass the magnetization drops sharply at T_m because of the SDW formation, while the magnetization of a conventional spin-glass reaches a maximum at zero temperature. The results presented here favor the interpretation of a conventional glass since field cooling always results in a susceptibility which is a maximum at zero temperature for low fields and is greater than the zero-field-cooled susceptibility for all fields.

High concentration samples exhibit long range antiferromagnetic order. The magnetic interactions are clearly different from the low-concentration samples. The susceptibility maximum is sharper and shows no field dependence. There are no mictomagnetic clusters formed in these samples. This may be due to crystallographic ordering at special compositions which form near

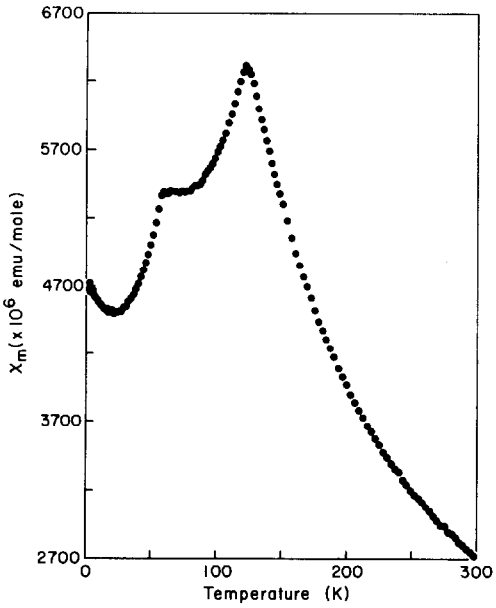

FIG. 10. Magnetic susceptibility vs temperature of $Fe_{0.40}TiSe_2$.

the percolation limit, which is estimated to be at $x = 0.20$. Arnaud *et al.* report a monoclinic supercell for $Fe_{0.25}TiS_2$ and more recently, Ibers *et al.* reported a hexagonal supercell for $Fe_{0.33}TiSe_2$. If the materials crystallographically order, clusters can not form and long range magnetic order is established, presumably through a superexchange mechanism.

Lyding *et al.* (*15*) report the magnetic ordering temperature for $Fe_{0.34}TiSe_2$ to be 113 K. The value obtained in this study is 61 K. The difference may be due to formation of a different superstructure. Several samples with the composition $Fe_{0.33}TiSe_2$ were prepared in this study and all had the same ordering temperature. Also, for samples with iron concentrations greater than $x = 0.25$, a disproportionation to the "special compositions" (1/4, 1/3, and 1/2) was observed. As seen in Fig. 10, the samples with $x = 0.40$, shows two susceptibility maxima, one corresponding to the $x = 0.33$ sample and the other corresponding to the $x = 0.50$ sample. The ordering temperature for the $Fe_{0.33}TiSe_2$ component of "$Fe_{0.40}TiSe_2$" is the same as the ordering temperature observed in the $Fe_{0.33}TiSe_2$ sample, indicating that under the reaction conditions used in this study, the stable $Fe_{0.33}TiSe_2$ phase is different than that prepared by Lyding.

In this study, magnetic susceptibility measurements suggest a transition from a spin-glass regime to an antiferromagnetic regime. The mechanism of ordering is likely to be a combination of superexchange and RKKY interactions, with superexchange being the most likely mechanism of ordering at high concentrations. The most definitive experiment to probe the magnetic structure would be neutron diffraction. The results also demonstrate that under certain reaction conditions, a disproportionation into two ordered phases is more stable than a high-concentration disordered material.

Acknowledgments

The research was supported by the National Science Foundation through Grant DMR 80-240050 and was supported in part by the AFOSR and the Materials Science Center at Cornell University. Thanks are also due to the Austrian Science Foundation for the use of the SUS-10 under Grant 4820. We gratefully acknowledge Professor R. Herber and T. McGuire for the Mössbauer data. D. H. thanks Dr. A. Stacy for help in the initial stages of this work.

References

1. A. D. YOFFE, *Ann. Chim. Fr.* **7**, 215 (1982).
2. J. VON BOEHM AND H. M. ISOMAKI, *J. Phys. C*, L733 (1982).
3. I. TAGUCHI, M. ASAI, Y. WATANABE, AND M. OKA, *Physica B* **105**, 146 (1981).
4. C. R. KANNEWURF, J. W. LYDING, M. T. RATAJACK, AND J. F. REVELLI, *in* "Ordering in Two Dimensions" (Sinha, Ed.), p. 403 (1980).
5. C. S. MCEWEN, M. R. HARRISON, D. R. HUNTLEY, AND M. J. SIENKO, *Inorg. Chem.*, submitted for publication.
6. S. S. P. PARKIN AND R. H. FRIEND, *Phil. Mag. B* **41(1)**, 65 (1980).
7. S. S. P. PARKIN AND R. H. FRIEND, *Phil. Mag. B* **41(1)**, 94 (1980).

8. O. GOROCHOV, A. LEBLANC-SOREAU, J. ROUXEL, P. IMBERT, AND G. JEHANNO, *Phil. Mag. B* **43(4),** 621 (1981).
9. J. J. BARRY AND H. P. HUGHES, *J. Phys. C, Solid State Phys.* **16,** L275 (1983).
10. D. A. WHITNEY, R. M. FLEMING, AND R. V. COLEMAN, *Phys. Rev. B* **15(7),** 3405 (1977).
11. S. J. HILENIUS, R. V. COLEMAN, E. R. DOMB, AND D. J. SELLMEYER, *Phys. Rev. B* **19(9),** 4711 (1979).
12. S. J. HILENIUS AND R. V. COLEMAN, *Phys. Rev. B* **20(11),** 4569 (1979).
13. M. DANOT, J. ROUXEL, AND O. GOROCHOV, *Mater. Res. Bull.* **9,** 1383 (1974).
14. T. TAKAHASHI AND O. YAMADA, *J. Solid State Chem.* **7,** 25 (1973).
15. J. W. LYDING, M. T. RATAJACK, C. R. KANNEWURF, W. H. GOODMAN, J. A. IBERS, AND R. E. MARSH, *J. Phys. Chem. Solids* **43(7),** 599 (1982).
16. S. MURANAKA AND T. TAKADA, *J. Solid State Chem.* **14,** 291 (1975).
17. Y. ARNAUD, M. CHEVRETON, A. AHOUANDJINOU, M. DANOT, AND J. ROUXEL, *J. Solid State Chem.* **18,** 9 (1976).
18. H. P. KLUG AND L. E. ALEXANDER, "X-Ray Diffraction Procedures," p. 574, Wiley–Interscience, New York (1974).
19. K. YVON, W. JEITSCHKO, AND E. PARTHE, *J. Appl. Crystallogr.* **10,** 73 (1977).
20. YOUNG, J. E. JR., Ph.D. thesis, Cornell Univ., (1973); modifications described: Johnson, D. C., Ph.D. thesis, Cornell Univ. (1984).
21. SUS-10: susceptibility measuring device, A. Paar KG, Graz, Austria.
22. C. RIEKEL, *J. Solid State Chem.* **17,** 389 (1976).
23. P. R. BEVINGTON, "Data Reduction and Error Analysis for the Physical Sciences," McGraw–Hill, New York (1969).
24. P. W. SELLWOOD, "Magnetochemistry," p. 78, Interscience, New York (1956).
25. R. HERBER AND T. MCGUIRE, private communication.
26. M. KATADA AND R. HERBER, *J. Solid State Chem.* **33,** 361 (1980).
27. P. FORD, *Contemp. Phys.* **23(2),** 141 (1982).
28. J. A. MYDOSH, G. J. NIEUWENHUYS, "Ferromagnetic Materials," Vol. 1, p. 71, North-Holland, Amsterdam (1980).
29. S. F. EDWARDS AND P. W. ANDERSON, *J. Phys. F, Met. Phys.* **5,** L49 (1975).
30. D. SHERRINGTON AND S. KIRKPATRICK, *Phys. Rev. Lett.* **35(26),** 1792 (1975).
31. D. J. THOULESS, P. W. ANDERSON, AND R. G. PALMER, *Phil. Mag.* **35(3),** 593 (1977).
32. A. W. OVERHAUSER, *J. Phys. Chem. Solids* **13,** 71 (1960).
33. P. D. ANTONIOU, *Phys. Rev. B* **20(1),** 231 (1979).